

Cite this: *Chem. Commun.*, 2012, **48**, 11948–11950

www.rsc.org/chemcomm

COMMUNICATION

Porous organic cage crystals: characterising the porous crystal surface†

Michael J. Bojdys,^a Tom Hasell,^a Nikolai Severin,^b Kim E. Jelfs,^a Jürgen P. Rabe^b and Andrew I. Cooper^{*a}

Received 11th September 2012, Accepted 15th October 2012

DOI: 10.1039/c2cc36602a

The characterisation of porous crystalline solids often relies on single crystal X-ray diffraction, which does not give direct information about the surface of the material. Here, crystals of a porous organic cage, CC3-R, are investigated by atomic force microscopy and shown to possess two distinct gas–solid interfaces, proving that the bulk crystal structure is preserved at the porous crystal surface.

Microporous, ordered solids such as zeolites,¹ metal–organic frameworks (MOFs)^{2,3} and organic polymer frameworks^{4–8} have excited much interest because of their potential contribution to more sustainable processes such as gas storage, molecular separation, and heterogeneous catalysis.^{9–12} These applications stem from the extraordinary surface-to-volume ratios of these materials, which show accessible surface areas ranging from several hundreds to a few thousands of square meters per gram. Also of interest are porous crystalline materials based on discrete, organic molecules, which can show surface areas exceeding 2000 m² g⁻¹,^{13,14} Unlike extended frameworks, porous organic molecules can be processed in solution and hence manipulated in the solid-state with relative ease,^{15–21} for example to form nanoparticles,^{22,23} hierarchically porous composites,²⁴ and thin porous layers for molecular sensors.²⁵ As with extended frameworks, porous molecular crystals have also been structurally characterized mostly by single crystal X-ray diffraction. However, in real applications, porous materials do not behave as ‘ideal’ crystals that can be represented solely by a repeating unit cell. In addition to the importance of crystal defects,²⁶ real materials have surfaces that are not represented in the single crystal structure. Moreover, the physical impact of surfaces – for example, in terms of guest uptake kinetics – will tend to become more pronounced as materials are reduced to the nanoscale.²² As such, the question of surface permeation in crystalline porous solids is important but has received relatively little attention. Confirming that the bulk crystal structure is

representative of the gas–solid interface becomes particularly relevant for coatings or membranes, where the interface-to-bulk-volume ratio is high. In such systems, the problem of additional surface resistance to molecular diffusion has been described previously as a “surface barrier”.^{27–31} Recently, periodic porous solids – for example, MOFs – have been investigated in the same context.^{26,32,33} In general, however, there is a gap in understanding in terms of the effect that the surface of such materials may play in terms of diffusion properties. The first step towards understanding this is to understand the nature of the material surface, and to confirm that it is representative of the bulk crystalline phase.

There is a maxim that nature tries to minimise surfaces or, more correctly, the potential energy of interfaces. However, porous crystals must necessarily present a porous surface: the question is whether or not this surface is representative of the bulk crystal structure. The microporous organic cage, CC3-R (Fig. 1a), is an octahedral, covalent, molecular pore formed *via* the [4 + 6] cyclocondensation reaction of (*R,R*)-1,2-diamino-cyclohexane and triformylbenzene.²⁰

The symmetry of this octahedral (or rectified tetrahedral) shaped molecule requires that opposing and neighbouring faces are alternatingly closed by the aryl group, or open in the form of a pore (Fig. 1b). It is interesting to note that this

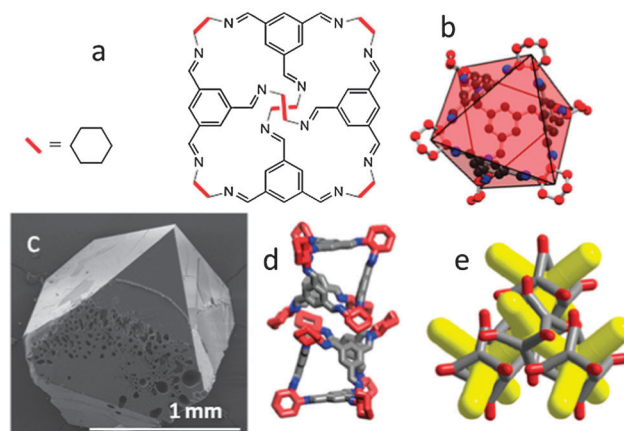


Fig. 1 (a) Chemical structure of CC3-R. (b) Molecular structure of CC3-R, with its octahedral shape emphasized. (c) Scanning electron microscope images of a crystal of CC3-R. (d) The window-to-window packing of the cages produces a diamondoid pore structure throughout the crystal. (e) The cyclohexyl vertices are highlighted in red in this scheme.

^a University of Liverpool, Department of Chemistry and Centre for Materials Discovery, Liverpool L69 7ZD, UK.

E-mail: aicooper@liverpool.com; Fax: +44 (0)151 794 2304; Tel: +44 (0)151 794 3548

^b Humboldt-Universität zu Berlin, Institut für Physik, Newtonstraße 15, 12489 Berlin, Germany. E-mail: rabe@physik.hu-berlin.de; Fax: +49 30 2093 7632; Tel: +49 30 2093 7621

† Electronic supplementary information (ESI) available: Synthetic procedures, Characterisation and modeling details, SEM and AFM images and analysis. See DOI: 10.1039/c2cc36602a

organic cage forms crystals that also have an octahedral or rectified tetrahedral morphology, mirroring the shape of the cage molecule itself (Fig. 1c) albeit 7 orders of magnitude larger (~ 1 nm diameter cage molecules *vs.* ~ 1 mm crystals). This crystal geometry can also be predicted by a Wulff plot, giving morphological importance to each face according to the Bravais–Friedel–Donnay–Harker law.²² Here, we show that the molecular geometry of **CC3-R** is not only replicated in the bulk crystal morphology, but it is also retained at the interfaces of its macroscopic crystals. Assessment of surface roughness by atomic force microscopy (AFM) reveals that geometric constraints of **CC3-R** dominate the supramolecular assembly at the crystal surface, rather than surface potential: that is, the surface structure is representative of the bulk crystal structure (Fig. 2).

The structure of the surfaces of **CC3-R** crystals was assessed by AFM on a representative number of crystallites and surfaces (see also Fig. S1 to S20, ESI†). Detailed scans of areas $20\text{ nm} \times 20\text{ nm}$ confirm the expected, principal repeat of about 1.8 nm in a hexagonal overlayer, corresponding to the average cage-to-cage distance, as established by single crystal X-ray diffraction. Depending on the cleanliness of the surface, some of the scans reveal additional, sub-molecular features (Fig. S18 to S20, ESI†). To interpret the observed topography, it is important to understand that the exposed, uppermost points of any of the accessible surfaces will be the cyclohexyl vertices, both in Miller planes $(-1\ -1\ -1)$ and $(1\ 1\ 1)$ (*cf.*, Fig. 2c, d and Fig. 3a, d). Models of the surface topography were constructed by cleaving the crystal to the respective Miller index and then generating the van der Waals surface. Geometry optimisation of the surfaces using a bespoke forcefield³⁴ showed no observable surface relaxation (see ESI† for full details). The surface was then coloured according to depth (*cf.*, Fig. 3a, d). The topography of Miller plane $(-1\ -1\ -1)$ is expected to have less pronounced differences between ‘hills’ and ‘valleys’ between cages, because the edges of the triangular windows fill out the inter-cage space, and the bottom of the inter-cage space is filled

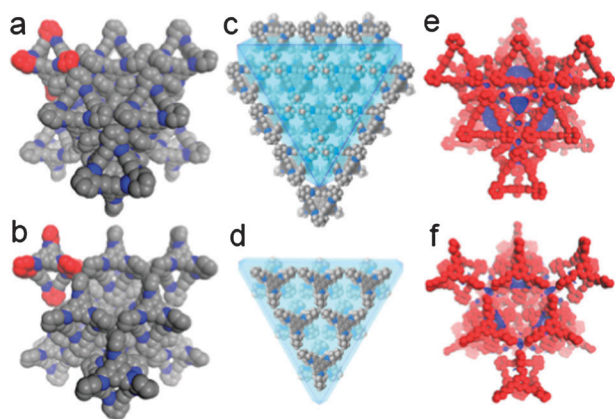


Fig. 2 (a–c) Predicted crystal planes with Miller indices $(-1\ -1\ -1)$ (a, c), and $(1\ 1\ 1)$ (b, d) shown as blue transparent triangles intersecting the top layer of cage molecules. Connolly surface plots (blue) with a probe radius of 1.82 \AA based on crystal structures for desolvated **CC3-R** (red), showing (d) the interconnected diamondoid pore channels, and the accessibility of these pore channels *via* (e) the $(-1\ -1\ -1)$ crystal plane and (f) the $(1\ 1\ 1)$ crystal plane.

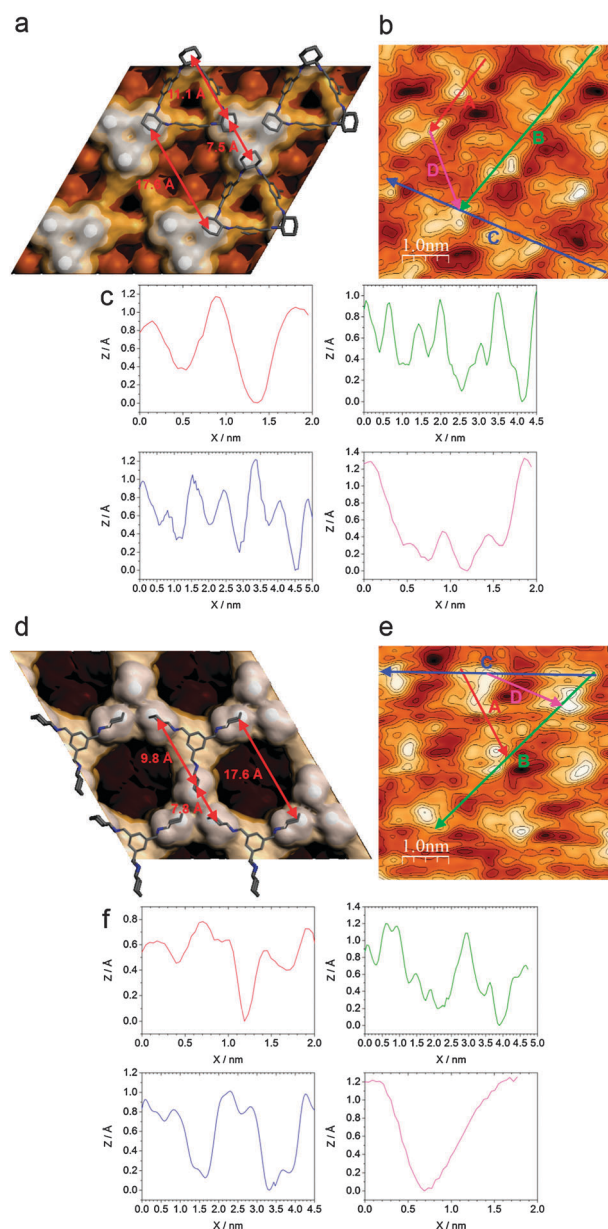


Fig. 3 Topographic study of **CC3-R** crystal surfaces. Modelled surface topographic based on a van der Waals surface of the crystal face along Miller plane (a) $(-1\ -1\ -1)$ and (d) $(1\ 1\ 1)$. Surface is coloured according to depth, with white for the uppermost part of the surface. Colours were changed every $1\text{--}1.5\text{ \AA}$. Top 4 \AA of the molecular lattice is superimposed as a guide for the eye. Indicated distances (in red) are measured between the most exposed atoms of the respective structures (based on X-ray crystallography). Software zoom on contact mode topography AFM images of the (b) $(-1\ -1\ -1)$ and (e) $(1\ 1\ 1)$ faces of **CC3-R**. Profile plots along the pathways A, B, C and D (in red, green, blue and pink) for the measured contact mode topography AFM images of the (c) $(-1\ -1\ -1)$ and (f) $(1\ 1\ 1)$ faces as seen in (b) and (e), respectively.

by the protruding cyclohexyl vertices of the atomic layer below (Fig. 3a). Miller plane $(1\ 1\ 1)$, on the other hand, shows triangular terraces spanned by the aryl faces and cyclohexyl vertices, interspersed by deep valleys of inter-cage space. This recess reaches all the way to down to the cyclohexyl vertices of

the same, uppermost layer of cages, which in this Miller plane point into the bulk of the crystal (Fig. 3d).

Topographic surveys of various surfaces and crystallites of CC3-*R* show two, qualitatively different surfaces on the crystal facets. Software zooms on the high-resolution contact mode topography AFM images of the $(-1\ -1\ -1)$ face (Fig. S18, ESI†) and the $(1\ 1\ 1)$ face (Fig. S19, ESI†) of CC3-*R* are shown in Fig. 3b and e, respectively. These contour maps are generated with WSxM 3.0 Scanning Probe Microscopy Software after Gaussian smoothing (X and Y decay distance of 5 matrix points) to account for the instrumental noise. The uppermost sub-molecular features appear as tri-fold ‘propellers’ (Fig. S18, S20, ESI† and Fig. 3b) and as round-edged triangles (Fig. S19, ESI† and Fig. 3e), which correspond to the cyclohexyl vertices of three neighbouring cages on the $(-1\ -1\ -1)$ face, and to the triangular terraces spanned by the aryl faces and cyclohexyl vertices on the $(1\ 1\ 1)$ face. Quantitative assessment of these topographic surveys should be made with caution due to the applied Gaussian smoothing of the raw data, and the intrinsic difficulties in judging the ‘highest’, most exposed features. However, qualitative profile plot analysis along selected paths on the surfaces corroborates the above assignment of Miller indices. Qualitative differences between ‘hills’ and ‘valleys’ in Fig. 3c are less pronounced than the deep recesses in Fig. 3f, which is in agreement with the topographic analysis based on van der Waals surface area plots (*cf.*, Fig. 3a and d). Likewise, the span of one tri-fold ‘propeller’ on the $(-1\ -1\ -1)$ plane of 0.7 to 0.8 nm (Fig. 3c) is smaller than the span of a round-edged, triangular plateau on the $(-1\ -1\ -1)$ plane of 0.9 to 1.1 nm (Fig. 3f), which is in good agreement with the crystallographic model (Fig. 3a and d; AFM lateral error \pm 0.05 nm).

In summary, we have shown that the geometry of the CC3-*R* cage molecule translates to bulk crystal structure and is retained at the crystal interface – that is, there is no evidence for alternative packing modes at the crystal surface, or for a ‘surface barrier’. However, this is not to say that the crystal surfaces are all the same in terms of structure and guest-transport properties. Two distinct types of interfaces, described by the Miller planes $(-1\ -1\ -1)$ and $(1\ 1\ 1)$, can be distinguished by AFM. It has been possible to observe the surface of the porous materials directly, which is shown to be in good agreement with the single crystal X-ray structure, proving that the surface does not relax or deviate from the bulk crystal packing in a way that would alter the sorption properties. This validates computational approaches that seek to simulate sorption properties for such materials using structures derived from single crystal X-ray diffraction, although we acknowledge that crystal defects, while not obvious in these AFM data, may still play an important role and that this is not captured by crystallography. We propose that these porous organic cage crystals might serve as model-systems to study surface permeability phenomena in microporous solids, in particular in the context of topical applications such as gas separation, and solution-processable porous membranes and coatings.

We thank EPSRC (EP/H000925/1) and the University of Liverpool for funding. A.I.C. is a Royal Society Wolfson Merit Award holder.

Notes and references

- P. A. Wright, *Microporous Framework Solids*, Royal Society of Chemistry, Cambridge, UK, 2008.
- S. Kitagawa, R. Kitaura and S. Noro, *Angew. Chem., Int. Ed.*, 2004, **43**, 2334–2375.
- S. R. Batten and R. Robson, *Angew. Chem., Int. Ed.*, 1998, **37**, 1460–1494.
- A. P. Cote, A. I. Benin, N. W. Ockwig, M. O’Keeffe, A. J. Matzger and O. M. Yaghi, *Science*, 2005, **310**, 1166–1170.
- H. Furukawa and O. M. Yaghi, *J. Am. Chem. Soc.*, 2009, **131**, 8875–8883.
- N. B. McKeown and P. M. Budd, *Chem. Soc. Rev.*, 2006, **35**, 675–683.
- P. Kuhn, A. Forget, D. Su, A. Thomas and M. Antonietti, *J. Am. Chem. Soc.*, 2008, **130**, 13333–13337.
- J. X. Jiang, F. Su, A. Trewin, C. D. Wood, N. L. Campbell, H. Niu, C. Dickinson, A. Y. Ganin, M. J. Rosseinsky, Y. Z. Khimyak and A. I. Cooper, *Angew. Chem., Int. Ed.*, 2007, **46**, 8574–8578.
- R. Dawson, A. I. Cooper and D. J. Adams, *Progr. Polym. Sci.*, 2012, **37**, 530–563.
- P. Kaur, J. T. Hupp and S. T. Nguyen, *ACS Catal.*, 2011, **1**, 819–835.
- F. Svec, J. Germain and J. M. J. Fréchet, *Small*, 2009, **5**, 1098–1111.
- A. Thomas, *Angew. Chem., Int. Ed.*, 2010, **49**, 8328–8344.
- M. Mastalerz, M. W. Schneider, I. M. Oppel and O. Presly, *Angew. Chem., Int. Ed.*, 2011, **50**, 1046–1051.
- M. W. Schneider, I. M. Oppel, H. Ott, L. G. Lechner, H.-J. S. Hauswald, R. Stoll and M. Mastalerz, *Chem.-Eur. J.*, 2012, **18**, 836–847.
- T. Hasell, M. Schmidtman and A. I. Cooper, *J. Am. Chem. Soc.*, 2011, **133**, 14920–14923.
- T. Hasell, M. Schmidtman, C. A. Stone, M. W. Smith and A. I. Cooper, *Chem. Commun.*, 2012, **48**, 4689–4691.
- J. T. A. Jones, T. Hasell, X. Wu, J. Bacsá, K. E. Jelfs, M. Schmidtman, S. Y. Chong, D. J. Adams, A. Trewin, F. Schiffrman, F. Cora, B. Slater, A. Steiner, G. M. Day and A. I. Cooper, *Nature*, 2011, **474**, 367–371.
- J. T. A. Jones, D. Holden, T. Mitra, T. Hasell, D. J. Adams, K. E. Jelfs, A. Trewin, D. J. Willock, G. M. Day, J. Bacsá, A. Steiner and A. I. Cooper, *Angew. Chem., Int. Ed.*, 2011, **50**, 749–753.
- N. B. McKeown, *J. Mater. Chem.*, 2010, **20**, 10588–10597.
- T. Tozawa, J. T. A. Jones, S. I. Swamy, S. Jiang, D. J. Adams, S. Shakespeare, R. Clowes, D. Bradshaw, T. Hasell, S. Y. Chong, C. Tang, S. Thompson, J. Parker, A. Trewin, J. Bacsá, A. M. Z. Slawin, A. Steiner and A. I. Cooper, *Nat. Mater.*, 2009, **8**, 973–978.
- T. Hasell, S. Y. Chong, M. Schmidtman, D. J. Adams and A. I. Cooper, *Angew. Chem., Int. Ed.*, 2012, **51**, 7154–7157.
- T. Hasell, S. Y. Chong, K. E. Jelfs, D. J. Adams and A. I. Cooper, *J. Am. Chem. Soc.*, 2012, **134**, 588–598.
- M. W. Schneider, L. G. Lechner and M. Mastalerz, *J. Mater. Chem.*, 2012, **22**, 7113–7116.
- T. Hasell, H. Zhang and A. I. Cooper, *Adv. Mater.*, 2012, DOI: 10.1002/adma.201202000.
- M. Brutschy, M. W. Schneider, M. Mastalerz and S. R. Waldvogel, *Adv. Mater.*, 2012, DOI: 10.1002/adma.201202786.
- F. Hibbe, C. Chmelik, L. Heinke, S. Pramanik, J. Li, D. M. Ruthven, D. Tzoulaki and J. R. Kärger, *J. Am. Chem. Soc.*, 2011, **133**, 2804–2807.
- A. Perret and F. Stoeckli, *Helv. Chim. Acta*, 1975, **58**, 2318–2321.
- D. D. Do, *Aiche J.*, 1989, **35**, 649–654.
- M. Bulow and A. Micke, *Adsorption*, 1995, **1**, 29–48.
- A. W. Harding, N. J. Foley, P. R. Norman, D. C. Francis and K. M. Thomas, *Langmuir*, 1998, **14**, 3858–3864.
- B. N. Nair, K. Keizer, W. J. Elferink, M. J. Gilde, H. Verweij and A. J. Burggraaf, *J. Membr. Sci.*, 1996, **116**, 161–169.
- S. Keskin and D. S. Sholl, *Langmuir*, 2009, **25**, 11786–11795.
- A. Micke, M. Bulow and M. Kocirik, *J. Phys. Chem.*, 1994, **98**, 924–929.
- D. Holden, K. E. Jelfs, A. I. Cooper, A. Trewin and D. J. Willock, *J. Phys. Chem. C*, 2012, **116**, 16639–16651.